Clinical Imaging 56 (2019) 52–57

Contents lists available at ScienceDirect

Clinical Imaging

journal homepage: www.elsevier.com/locate/clinimag

Pediatric Radiology

Protocol optimization for cardiac and liver iron content assessment using MRI: What sequence should I use?

Christian A. Barrera[a,*], Hansel J. Otero[a], Helge D. Hartung[b], David M. Biko[a], Suraj D. Serai[a]

[a] Department of Radiology, The Children's Hospital of Philadelphia, 34th Street & Civic Center Boulevard, Philadelphia, PA 19104, USA
[b] Department of Pediatrics, The Children's Hospital of Philadelphia, 34th Street & Civic Center Boulevard, Philadelphia, PA 19104, USA

ARTICLE INFO

Keywords:
Children
MRI
T2 star
T2
Liver
Heart
Protocol

ABSTRACT

Objective: To determine the optimal MRI protocol and sequences for liver and cardiac iron estimation in children.

Methods: We evaluated patients ≤18 years with cardiac and liver MRIs for iron content estimation. Liver T2 was determined by a third-party company. Cardiac and Liver T2* values were measured by an observer. Liver T2* values were calculated using the available liver parenchyma in the cardiac MRI. Linear correlations and Bland-Altman plots were run between liver T2 and T2*, cardiac T2* values; and liver T2* on dedicated cardiac and liver MRIs.

Results: 139 patients were included. Mean liver T2 and T2* values were 8.6 ± 5.4 ms and 4.5 ± 4.1 ms, respectively. A strong correlation between liver T2 and T2* values was observed ($r = 0.96$, $p < 0.001$) with a bias (+4.1 ms). Mean cardiac bright- and dark-blood T2* values were 26.5 ± 12.9 ms and 27.2 ± 11.9 ms, respectively. Cardiac T2* values showed a strong correlation ($r = 0.81$, $p < 0.001$) with a low bias (−1.0 ms). The mean liver T2* on liver and cardiac MRIs were 4.9 ± 4.7 ms and 4.6 ± 3.9 ms, respectively. A strong correlation between T2* values was observed ($r = 0.96$, $p < 0.001$) with a small bias (−0.2 ms).

Conclusion: MRI protocols for iron concentration in the liver and the heart can be simplified to avoid redundant information and reduce scan time. In most patients, a single breath-hold GRE sequence can be used to evaluate the iron concentration in both the liver and heart.

1. Introduction

Iron is an essential element present throughout the body in different tissues and cells [1]. Conditions that increase intestinal iron absorption (e.g. hereditary hemochromatosis) or require chronic intravenous blood transfusions (e.g. sickle cell anemia post stroke or thalassemia major) are related to iron overload in children [1]. Iron affects multiple organs but the heart and the liver are at the highest risk for toxicity with the liver typically being the first organ affected given that it is the main iron storage in the body [2,3].

Magnetic resonance imaging (MRI) has been used to detect iron deposits for > 25 years and has revolutionized clinical care of conditions that result in iron overload [4,5]. In the liver, the most validated and widely used relaxometry methods for iron quantification are R2 and R2* [6]. These techniques are based on T2 and T2* sequences, respectively. Although both are validated to estimate the liver iron content (LIC), few studies have analyzed the correlation between both sequences [9,10]. For the heart, bright-blood (BB) and dark-blood (DB) T2* sequences are used to evaluate response to chronic iron chelation in clinical practice [11–13]. DB-T2* suppresses the signal comping from the blood, improves myocardium depiction and facilitates the post-processing [12].

In current clinical practice, in order to estimate cardiac and hepatic iron content, we require separate MRIs with sequences tailored specifically for each organ. This workflow results in multiple redundant scans and unnecessarily long examinations. However, a large part of the liver is included in the field of view during the cardiac MRI and can potentially be used to estimate the LIC using any of the T2* sequences. Optimization of this MRI protocol could reduce expenses and scanner time while improving the patient experience without losing diagnostic value. This retrospective study aims to compare the different sequences for liver and cardiac iron estimation in children. In this study, we compared different T2 and T2* sequences for iron estimation in the liver and heart.

* Corresponding author at: 34th Street & Civic Center Boulevard, USA.
E-mail address: barreracac@email.chop.edu (C.A. Barrera).

https://doi.org/10.1016/j.clinimag.2019.02.012
Received 17 December 2018; Received in revised form 31 January 2019; Accepted 19 February 2019

2. Materials and methods

This retrospective study was approved by our Institutional Review Board and performed in compliance with the Health Insurance Portability and Accountability Act. The requirements for informed consent and assent were waived. Patients aged 0–18 years old who had both a liver and a cardiac MRI indicated for iron overload assessment between February 2008 and December 2017 were included. Liver and cardiac MRIs were performed < 90 days apart to ensure comparability. During the first years of this period, the cardiac and liver MRIs were performed at different days according to the patient's preference or lack of availability during the day. Currently, at our institute, cardiac and liver MRIs are preferably performed one after the other the same day. Patients whose cardiac MRI did not have an adequate technique to estimate the LIC and those who did not included the liver in the cardiac MRI field of view for any given reason were excluded. Demographic and anthropometric measures in addition to MRI scanner parameters were retrieved from the electronic medical records. All liver and cardiac scans were performed using a 1.5 T MRI scanner (Avanto, Siemens Health Care, Erlangen, Germany) equipped with a gradient system with a maximum amplitude of 33 mT/m and a 125 mT/m/ms slew rate. Imaging sequence and coils were constant between 2008 and 2017. MR software was updated in 2011, 2016 and 2017 but without changes in the liver or cardiac iron quantification protocol. An acquired matrix size without reconstruction was used. Scanner parameters used for the liver T2, liver T2* and cardiac T2* MRI sequences are shown in Table 1. DB-T2* uses a double inversion recovery pulse to null the signal coming from the blood.

T2 calculations were done based on methodology reported by St. Pierre et al [7,14]. The transverse relaxation rate, T2, was calculated by exponential curve fitting to the image signal intensities obtained by the TE images. For LIC, a litter of saline solution bag was placed to the left side of the torso as a reference for correction of signal gain changes. The mean T2 values within the liver was used to calculate a mean LIC using a calibration curve that had been determined through the measurements of liver T2 and needle biopsy [7]. The image analysis for LIC values using T2 values was performed offline by Resonance Health (Claremont, Australia) for a fee per study using FDA approved methodology. After analysis, a report was sent back to our institution. LIC calculated from T2 sequences plateaus at 43 mg/g and values beyond this cut-off were not reported. In order to calculate T2*, all MRI images were transferred to a post-processing program (Circle Cardiovascular Imaging 42, version 5.6.5, Calgary, AB, Canada). A single trained observer supervised by a physicist with 15 years of experience in MR imaging drew the regions of interest (ROI) in the heart and liver. Liver ROIs were drawn on the liver parenchyma encompassing the relevant anatomy in the right hepatic lobe with special care taken to avoid major vessels, central biliary tree, artifacts and livers boundaries. Normal liver iron content is 0.2–2 mg Fe/g dry weight [2]. Cardiac ROIs were drawn delineating the mid-interventricular septum and excluding any surrounding blood. ROIs size varied among the patients based on the liver and heart size, orientation and position of large vascular structures. Unlike liver MRI that calculates the LIC, cardiac iron overload is evaluated using the T2* values (ms) themselves instead of the iron content [15]. The ROIs in the liver using a dedicated cardiac MRI were drawn in the sagittal view encompassing as much liver as possible while avoiding the large vascular structures in the mid-liver, usually the left hepatic lobe, and with a size comparable to the ROI drawn in the dedicated liver MRI, Fig. 1. As the software propagates the ROI automatically to the other TE acquisitions of the series, it generates a decay curve and calculates the T2* value in milliseconds for the ROI. A single exponential curve fitting was used for T2* decay curve fitting. In cases with rapid signal decay, the curve fitting fails with the current number of echoes. In these cases, the curve was corrected by excluding later echoes as they were considered noise. The minimum number of echoes necessary to achieve and acceptable curve fitting were excluded in these patients. In addition, eight examinations were excluded because the first TE in the dedicated cardiac exam was insufficiently short for the high degree of liver iron overload and yield a failed curve fitting. By default, the first TE in the cardiac MRI were shorter as compared to the liver MRI.

Statistical analyses were performed using MedCalc (MedCalc, Ostend, Belgium). Continuous variables were presented as mean ± standard deviation (SD) and categorical variables as percentages and counts. Linear correlation (r) was done to evaluate the relationship between liver T2 vs. liver T2*, cardiac BB- vs DB- T2* and liver T2* obtained on dedicated liver MRI vs. cardiac MRI. 95% confidence intervals (95% CI) for each correlation were calculated. Scatter plots and Bland-Altman difference plots were calculated to assess the agreement between the two methods. 95% confidence intervals were used as prediction limit in order to identify and display outliers. A two-tailed p-value of < 0.05 was considered significant.

Table 1
Pulse sequence parameters for T2 and T2* sequences used for liver and cardiac MRI.

Parameter	T2 Liver MRI	T2* Liver MRI	T2* Cardiac MRI
Type of sequence	Spin Echo (SE)	Gradient Echo (GRE)	Gradient Echo (GRE)
Scan mode	2D	2D	2D
TR (ms)	1000	200	120
No. of echoes	5	12	8
First TE value (ms)	6	1	2.5
Echo space (ms)	3	1.4	2.2
Flip angle	90	20	20
Matrix size	256 × 256	128 × 64	256 × 192
Slice thickness (mm)	6	10	10
No. of slices	11	2	2
Acceleration factor	2	2	2
Approx. Scan time (min:sec)	10:00	0:18	0:17

Note: TE = Echo time, TR = Repetition time, ms = milliseconds.

3. Results

139 patients (87 Girls, 52 Boys) were included with a mean age, weight and height of 12.5 ± 3.7 years (range 2–18), 42.5 ± 16.7 kg (range 12.2–116.5) and 143.4 ± 20.3 cm (range 67.8–181.8). 74.8% of the abdominal and cardiac MRI studies were performed on the same day and 4.3% one day apart. 20.8% of our studies were performed between 4 and 74 days apart with a mean 26.1 ± 19.3 days. Diagnoses seen in our sample were beta-thalassemia (n = 88), sickle cell disease (n = 16), sideroblastic anemia (n = 14), pyruvate kinase deficiency (n = 3), aplastic anemia (n = 3), acute lymphoblastic leukemia (n = 5), alpha thalassemia (n = 3), Diamond-Blackfan anemia (n = 4), hereditary spherocytosis (n = 1), Langerhans cell histiocytosis (n = 1) and hemolytic anemia of uncertain ethology (n = 1).

139 MRIs were included to compare T2 and T2*. The mean T2 and T2* were 8.6 ± 5.4 ms and 4.5 ± 4.1 ms, respectively. LIC values were 16.6 ± 13.4 mg/g (range 1–43) for T2 and 15.7 ± 12.7 mg/g (range 1.02–47.9) for T2*. A strong correlation was observed between T2 and T2* values (r = 0.96, 95% CI 0.94–0.97, $p < 0.001$). Bland-Altman plot depicts a mean bias of +4.1 ms (range + 0.4 to +7.7) between T2 and T2* values. With the exception of six outliers, all values fall within 95% prediction limits, Fig. 2.

Out of 139 patients, 99 subjects had a cardiac MRI with both BB- and DB-T2* sequences acquired in the same examination. The mean BB- and DB-T2* values were 26.3 ± 12.9 ms and 27.23 ± 11.9 ms, respectively. Regression analysis between BB- and DB-T2* showed a strong correlation (r = 0.81, 95% CI 0.73–0.86, $p < 0.001$). Bland-Altman plot shows the mean bias between BB- and DB-T2* was – 0.6 ms (range – 15.6 ms to +14.3 ms), Fig. 3. Except for two outliers, all values

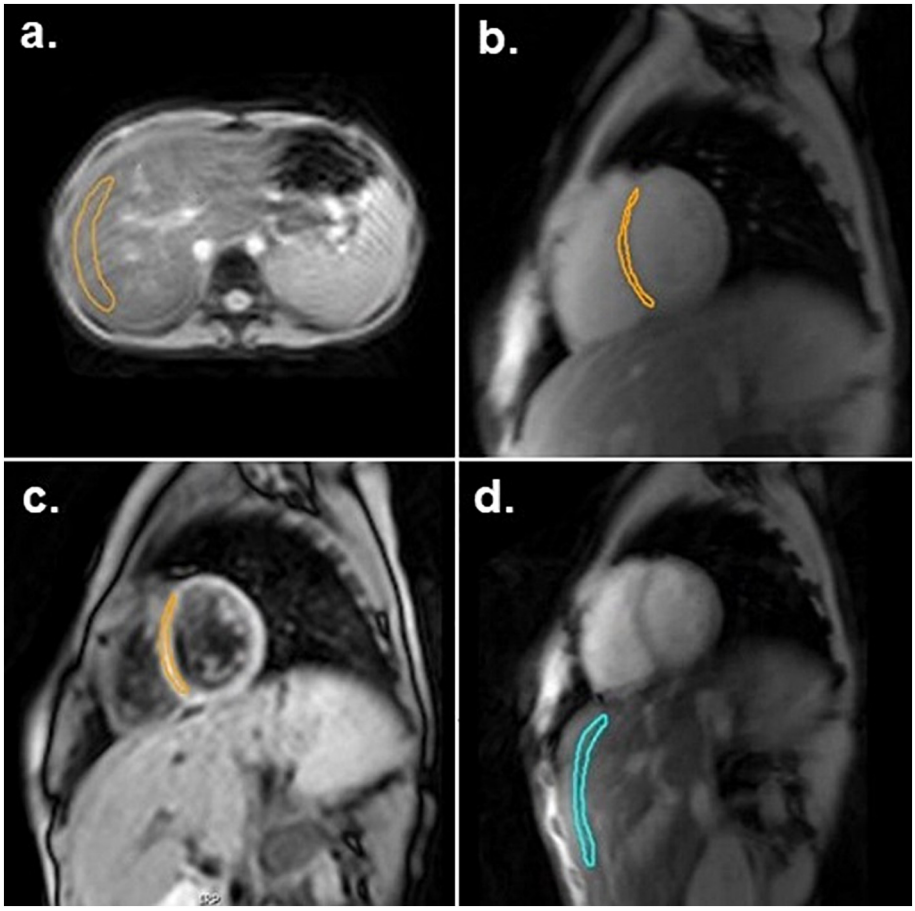

Fig. 1. Representation of ROIs used for T2* estimation in the liver and heart. A single trainee draw an ROI in the right hepatic lobe using the dedicated liver MRI (a), bright blood (b) and dark blood sequences delineating the mid-interventricular septum (c); and in the mid-liver using a dedicated cardiac MRI (d).

fall within 95% prediction limits.

Out of 139 patients, 131 cardiac MRIs were included to measure the liver T2* in the liver and cardiac MRIs. The mean T2* values measured on the liver and cardiac MRIs were 4.9 ± 4.7 ms and 4.6 ± 3.9 ms, respectively. Regression analysis between liver T2* measured in the cardiac and liver MRI showed a strong correlation (r = 0.96, 95% CI 0.94–0.97, $p < 0.001$), Fig. 4. Based on Bland-Altman plots, the mean bias in liver T2* measured between the cardiac and liver MRI is – 0.2 ms (range – 2.3 ms to +1.8 ms). Most of our values fall within 95% prediction limits, with the exception of three outliers.

4. Discussion

Our findings support an MR protocol for evaluation of iron overload in the liver and heart in children limited to a single sequence acquisition. We compared multiple sequences to determine an optimal approach that improves the MR imaging experience and facilitates follow-up in patients with iron overload. Previous studies evaluated this approach with similar results [16,17].

While there are multiple MR sequences that allow the estimation of liver and cardiac iron content, T2 and T2* currently dominate the market [18]. Wood et al and Serai SD et al found good consistency and agreement between both sequences in the liver [9,10]. Similarly, T2* measurements have an excellent inter-obverse variability between ROIs [19]. Although a third-party company performed the T2 measurements, a previous study showed an excellent agreement between the proprietary and non-proprietary methods [20]. However, it is important to acknowledge that individual institutions might have traditionally opted for a separate liver iron concentration sequence based on a low number of patients per year or lack of acquisition or post-processing expertise.

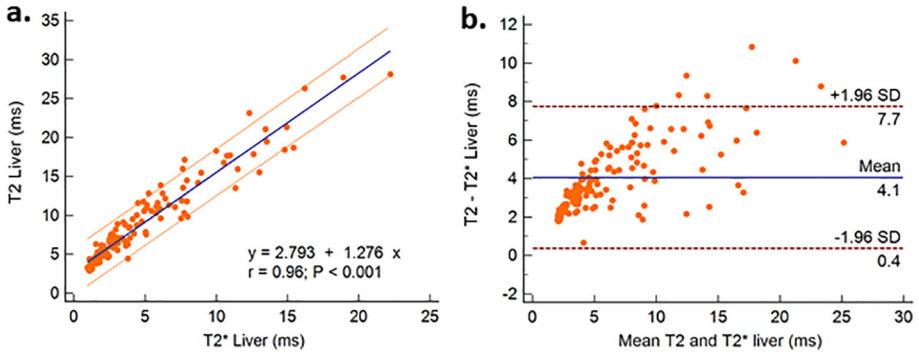

Fig. 2. Scatterplot shows the correlation between liver T2 and T2* values. Solid blue line is the line of best fit with the dotted red lines representing the 95% prediction limits for the best-fit line. (r = 0.96, $R^2 = 0.91$). Bland-Altman plot shows a low bias of +4.1 between T2 and T2*. Except for six outlier, all measurements fall within two standard deviations. (For interpretation of the references to color in this figure legend, the reader is referred to the web version of this article.)

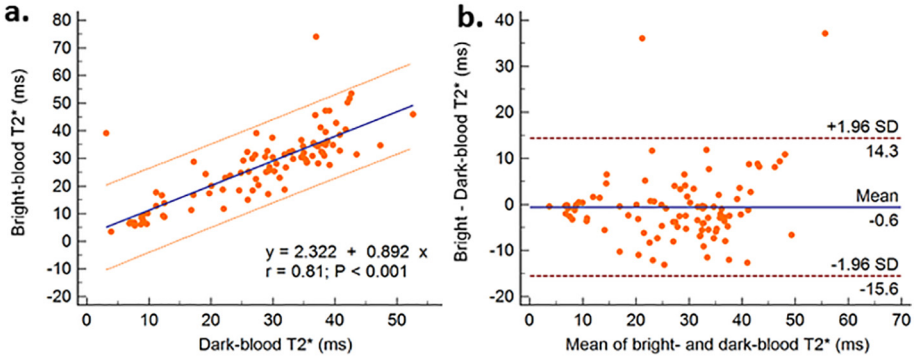

Fig. 3. Scatterplot shows the correlation between cardiac T2* bright- and dark-blood. Solid blue line is the line of best fit with the dotted red lines representing the 95% prediction limits for the best fit line (r = 0.81, R^2 = 0.66). Bland-Altman plot shows a mean bias of – 0.6 ms between bright- and dark-blood T2* sequences. Except for two outliers, all measurements fall within two standard deviations. (For interpretation of the references to color in this figure legend, the reader is referred to the web version of this article.)

T2 is less sensitive to external magnetic in-homogeneities, technical variation, artifacts and non-iron related confounding factors such as metal clips [21]. In addition, data analysis, phantom's calibration and quality control evaluations are centralize [9], which might be advantageous for centers with low patient volume. T2* data acquisition is relatively faster than T2 and less susceptible to variations in iron distribution and deposits size but requires trained staff to perform the post-processing. T2* is performed in a single breath hold of 10 to 15 s, compared to T2 which takes around 10 to 15 min [2,9,22,23]. However, both techniques loose accuracy in patients with severe iron overload because the signal decay is faster than the echo acquisition times [2,7,24]. The dynamic range of LIC for T2 values is around 0–43 mg/g and for T2* is usually around 0–35 mg/g [9,13]. Under current standards, patients with severe iron overload might not be able to benefit from a single acquisition because cardiac T2* GRE sequence use a slightly higher minimum TE compared to liver protocols. This was the case for eight studies in our sample, which were excluded from the analysis because the first TE in the cardiac MRI parameters was not short enough to calculate the LIC. These patients would benefit from ultrashort first echo time sequences in which the first echo time is short enough to capture initial signal decay (TE < 1 ms.) [8,25,26]. Recent studies with ultra-short echo time images are based on T2* relaxometry which may be an additional advantage to choose T2* over T2 once this sequence starts to be use clinically [25,26]. New MR techniques, such as quantitative susceptibility mapping and multi-echo Dixon based methods such as mDixon/IDEAL-IQ, are based on corrected T2* sequences with the advantage of being unaffected by confounding factors like fat, fibrosis and edema. This makes these modern techniques more suitable to determine the iron concentration in the liver and heart [27–29]. In a recent study, Serai et al, validated 3D mDixon with 2D relaxometry based measurements as an accurate method for measuring liver T2* [30]. Additional large scale multi-center studies are needed to validate these findings before these newer methods can be translated to routine clinical use.

Dark blood- performed as well as bright-blood T2* with the advantage of improving visualization by overcoming blood-related artifacts [12]. Previous studies showed DB-T2* offers better inter-observer, intra-observer and inter-study reproducibility [31–34]. Although we found a strong correlation between DB- and BD-T2* values, we expected better results given that these sequences are almost identical. However, artifacts and low signal contrast between blood and myocardium on BD-T2* can be detrimental during the post-processing [12]. DB-T2* sequences yield fewer motion, blood flow and partial volume artifacts with better myocardial delineation which improves analysis [35]. One disadvantage to the DB-T2* sequence is that it requires slightly more time to achieve blood signal nulling. However, based on our clinical experience, motion artifacts with DB-T2* do not significantly affect the analysis and is preferred for clinical use over BB-T2* sequences [36]. Early studies used T2 sequences to quantify iron in the heart; but, these measurements were unsatisfactory due to hardware constrains and motion artifacts. [37,38]. We hope that our results help build upon existing evidence on the feasibility and benefits of T2* relaxometry for iron content estimation during cardiac MRI.

A single sequence to assess iron concentration in the heart and the liver based on T2* sequences is feasible and might benefit even more those patients unable to tolerate longer examination times and those that require sedation. However, even in the absence of contraindications to longer or repeat exams, a single acquisition would improve the overall experience and potentially save additional direct (e.g.; billing for the individual exams) and indirect (e.g.; lost wages for caregivers, transportation cost or school absenteeism). A single acquisition requires additional training to the MR technologist to avoid know albeit rare pitfalls such as imaging liver transplant recipients and those with massive splenomegaly, which might need a second sequence with extended coverage of the liver. In our sample, one patient had massive splenomegaly, which displaced the liver to the right and downwards and led to exclude enough hepatic parenchyma for LIC analysis. Finally, liver iron deposition is heterogeneous throughout the liver parenchyma; commonly showing as lower T2* values in the right hepatic lobe (segments VII and VIII) compared to the rest of the liver parenchyma [19,39]. However, most of the liver observed through the cardiac acquisition belongs to the left hepatic lobe. Hence, this is not a

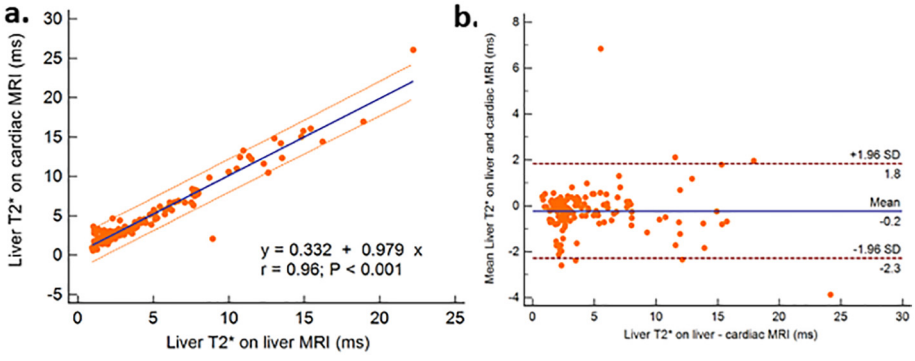

Fig. 4. Scatterplot shows the correlation between liver T2* values obtained on the dedicated cardiac MRI vs. liver T2* values obtained on the dedicated liver MRI. Solid blue line is the line of best fit with the dotted red lines representing the 95% prediction limits for the best fit line (r = 0.96, R^2 = 0.94). Bland-Altman plot shows a low bias of – 0.2 ms between liver T2* values obtained on the dedicated cardiac MRI vs. liver T2* values obtained on the dedicated liver MRI. Except for three borderline outliers, all measurements fall within two standard deviations. (For interpretation of the references to color in this figure legend, the reader is referred to the web version of this article.)

problem for new patients but an adjustment might be needed in those patients in whom a single acquisition (i.e.; left hepatic lobe) data is acquired and then compared to historic values in the right hepatic lobe. Previous studies reported similar issues when estimating the LIC using a cardiac MRI [16,17].

Going forward, relatively simple adjustments to the protocol, especially regarding the field of view, could allow to measure T2* values in the pancreas which showed to help to predict endocrine dysfunction [13,40].

Our study has few limitations. First, we did not have concurrent liver biopsies to compare with the MRI results. However, MRI is well established and is highly correlated with LIC obtained by biopsy [10,41]. Conversely, liver biopsy showed more sampling error compared to T2 and T2* values in patients on iron chelation [42]. Additionally, current clinical standards and guidelines no longer recommend liver biopsy for routine evaluation of LIC. Second, this is a retrospective study and as such limited to the available medical records and MRI studies from a defined spectrum of diagnoses. For example, approximately half of our subjects have beta-thalassemia and it is well known that iron overload rate and pattern changes according to the underlying condition [2]. Third, ROIs were drawn only by one observed instead of multiple measurements by two or more observers. However, previous studies showed excellent inter-observer and intra-observer reproducibility between T2 and T2* measurements [9,32]. Moreover, a single trained user probably more closely resembles standard clinical practice in most imaging centers. Finally, the cardiac T2* GRE sequences (either bright or dark blood) used for LIC measurement was not optimized for this purpose. However, given our encouraging results, minimal modifications (such as lower initial TE to accommodate patients with high LIC and education to the performing MRI technologists and supervisors to ensure appropriate coverage) could lead to a more robust performance of a single acquisition approach.

5. Conclusion

In conclusion, MRI protocols for iron concentration in the liver and the heart can be simplified to avoid redundant information and reduce scan time. In most patients, a single breath-hold GRE sequence can be used to evaluate the iron concentration in both the liver and heart.

Conflict of interest

The authors declare that they have no conflict of interest.

References

[1] Lieu PT, Heiskala M, Peterson PA, Yang Y. The roles of iron in health and disease. Mol Aspects Med 2001;22(1):1–87.
[2] Sirlin CB, Reeder SB. Magnetic resonance imaging quantification of liver iron. Magn Reson Imaging Clin N Am 2010;18(3):359–81. [ix].
[3] Angelucci E, Brittenham GM, McLaren CE, Ripalti M, Baronciani D, Giardini C, et al. Hepatic iron concentration and total body iron stores in thalassemia major. N Engl J Med 2000;343(5):327–31.
[4] Bassett ML, Halliday JW, Powell LW. Value of hepatic iron measurements in early hemochromatosis and determination of the critical iron level associated with fibrosis. Hepatology (Baltimore, MD) 1986;6(1):24–9.
[5] Stark DD, Goldberg HI, Moss AA, Bass NM. Chronic liver disease: evaluation by magnetic resonance. Radiology 1984;150(1):149–51.
[6] Towbin AJ, Serai SD, Podberesky DJ. Magnetic resonance imaging of the pediatric liver: imaging of steatosis, iron deposition, and fibrosis. Magn Reson Imaging Clin N Am 2013;21(4):669–80.
[7] St Pierre TG, Clark PR, Chua-anusorn W, Fleming AJ, Jeffrey GP, Olynyk JK, et al. Noninvasive measurement and imaging of liver iron concentrations using proton magnetic resonance. Blood 2005;105(2):855–61.
[8] Chappell KE, Patel N, Gatehouse PD, Main J, Puri BK, Taylor-Robinson SD, et al. Magnetic resonance imaging of the liver with ultrashort TE (UTE) pulse sequences. J Magn Reson Imaging 2003;18(6):709–13.
[9] Serai SD, Fleck RJ, Quinn CT, Zhang B, Podberesky DJ. Retrospective comparison of gradient recalled echo R2* and spin-echo R2 magnetic resonance analysis methods for estimating liver iron content in children and adolescents. Pediatr Radiol 2015;45(11):1629–34.
[10] Wood JC, Enriquez C, Ghugre N, Tyzka JM, Carson S, Nelson MD, et al. MRI R2 and R2* mapping accurately estimates hepatic iron concentration in transfusion-dependent thalassemia and sickle cell disease patients. Blood 2005;106(4):1460–5.
[11] Westwood M, Anderson LJ, Firmin DN, Gatehouse PD, Charrier CC, Wonke B, et al. A single breath-hold multiecho T2* cardiovascular magnetic resonance technique for diagnosis of myocardial iron overload. J Magn Reson Imaging 2003;18(1):33–9.
[12] He T. Cardiovascular magnetic resonance T2* for tissue iron assessment in the heart. Quant Imaging Med Surg 2014;4(5):407–12.
[13] Wood JC. Use of magnetic resonance imaging to monitor iron overload. Hematol Oncol Clin North Am 2014;28(4):747–64.
[14] St Pierre TG, Clark PR, Chua-Anusorn W. Measurement and mapping of liver iron concentrations using magnetic resonance imaging. Ann N Y Acad Sci 2005;1054:379–85.
[15] Pennell DJ, Udelson JE, Arai AE, Bozkurt B, Cohen AR, Galanello R, et al. Cardiovascular function and treatment in beta-thalassemia major: a consensus statement from the American Heart Association. Circulation 2013;128(3):281–308.
[16] Serai SD, Trout AT, Fleck RJ, Quinn CT, Dillman JR. Measuring liver T2* and cardiac T2* in a single acquisition. Abdominal Radiology (New York). 2018.
[17] Tan S, Peng Q, Liszewski MC, Taragin BH. From the bottom of the heart: measuring liver iron concentration on cardiac MRI. Clin Imaging 2018;47:124–9.
[18] Labranche R, Gilbert G, Cerny M, Vu KN, Soulieres D, Olivie D, et al. Liver Iron quantification with MR imaging: a primer for radiologists. Radiographics 2018;38(2):392–412.
[19] McCarville MB, Hillenbrand CM, Loeffler RB, Smeltzer MP, Song R, Li CS, et al. Comparison of whole liver and small region-of-interest measurements of MRI liver R2* in children with iron overload. Pediatr Radiol 2010;40(8):1360–7.
[20] Pirasteh A, Yuan Q, Hernando D, Reeder SB, Pedrosa I, Yokoo T. Inter-method reproducibility of biexponential R2 MR relaxometry for estimation of liver iron concentration. Magn Reson Med 2018;80(6):2691–701.
[21] St Pierre TG, Clark PR, Chua-Anusorn W. Single spin-echo proton transverse relaxometry of iron-loaded liver. NMR Biomed 2004;17(7):446–58.
[22] Brewer CJ, Coates TD, Wood JC. Spleen R2 and R2* in iron-overloaded patients with sickle cell disease and thalassemia major. J Magn Reson Imaging 2009;29(2):357–64.
[23] Chandarana H, Lim RP, Jensen JH, Hajdu CH, Losada M, Babb JS, et al. Hepatic iron deposition in patients with liver disease: preliminary experience with breath-hold multiecho T2*-weighted sequence. AJR Am J Roentgenol 2009;193(5):1261–7.
[24] Tanimoto A, Oshio K, Suematsu M, Pouliquen D, Stark DD. Relaxation effects of clustered particles. J Magn Reson Imaging 2001;14(1):72–7.
[25] Doyle EK, Toy K, Valdez B, Chia JM, Coates T, Wood JC. Ultra-short echo time images quantify high liver iron. Magn Reson Med 2018;79(3):1579–85.
[26] Krafft AJ, Loeffler RB, Song R, Tipirneni-Sajja A, McCarville MB, Robson MD, et al. Quantitative ultrashort echo time imaging for assessment of massive iron overload at 1.5 and 3 Tesla. Magn Reson Med 2017;78(5):1839–51.
[27] Sharma SD, Fischer R, Schoennagel BP, Nielsen P, Kooijman H, Yamamura J, et al. MRI-based quantitative susceptibility mapping (QSM) and R2* mapping of liver iron overload: comparison with SQUID-based biomagnetic liver susceptometry. Magn Reson Med 2017;78(1):264–70.
[28] Dong J, Liu T, Chen F, Zhou D, Dimov A, Raj A, et al. Simultaneous phase unwrapping and removal of chemical shift (SPURS) using graph cuts: application in quantitative susceptibility mapping. IEEE Trans Med Imaging 2015;34(2):531–40.
[29] Hernando D, Kramer JH, Reeder SB. Multipeak fat-corrected complex R2* relaxometry: theory, optimization, and clinical validation. Magn Reson Med 2013;70(5):1319–31.
[30] Serai SD, Smith EA, Trout AT, Dillman JR. Agreement between manual relaxometry and semi-automated scanner-based multi-echo Dixon technique for measuring liver T2* in a pediatric and young adult population. Pediatr Radiol 2018;48(1):94–100.
[31] Smith GC, Carpenter JP, He T, Alam MH, Firmin DN, Pennell DJ. Value of black blood T2* cardiovascular magnetic resonance. J Cardiovasc Magn Reson 2011;13:21.
[32] Liguori C, Di Giampietro I, Pitocco F, De Vivo AE, Schena E, Mortato L, et al. Dark blood versus bright blood T2 acquisition in cardiovascular magnetic resonance (CMR) for thalassaemia major (TM) patients: evaluation of feasibility, reproducibility and image quality. Eur J Radiol 2014;83(1):e8–14.
[33] He T, Gatehouse PD, Kirk P, Tanner MA, Smith GC, Keegan J, et al. Black-blood T2* technique for myocardial iron measurement in thalassemia. J Magn Reson Imaging 2007;25(6):1205–9.
[34] Kirk P, He T, Anderson LJ, Roughton M, Tanner MA, Lam WW, et al. International reproducibility of single breathhold T2* MR for cardiac and liver iron assessment among five thalassemia centers. J Magn Reson Imaging 2010;32(2):315–9.
[35] Carpenter JP, He T, Kirk P, Roughton M, Anderson LJ, de Noronha SV, et al. On T2* magnetic resonance and cardiac iron. Circulation 2011;123(14):1519–28.
[36] Messroghli DR, Moon JC, Ferreira VM, Grosse-Wortmann L, He T, Kellman P, et al. Clinical recommendations for cardiovascular magnetic resonance mapping of T1, T2, T2* and extracellular volume: a consensus statement by the Society for Cardiovascular Magnetic Resonance (SCMR) endorsed by the European Association for Cardiovascular Imaging (EACVI). J Cardiovasc Magn Reson 2017;19(1):75.
[37] Mavrogeni SI, Gotsis ED, Markussis V, Tsekos N, Politis C, Vretou E, et al. T2 relaxation time study of iron overload in b-thalassemia. Magma (New York, NY) 1998;6(1):7–12.
[38] Papanikolaou N, Ghiatas A, Kattamis A, Ladis C, Kritikos N, Kattamis C. Non-invasive myocardial iron assessment in thalassaemic patients. T2 relaxometry and magnetization transfer ratio measurements. Acta Radiol 2000;41(4):348–51.
[39] Meloni A, Luciani A, Positano V, De Marchi D, Valeri G, Restaino G, et al. Single region of interest versus multislice T2* MRI approach for the quantification of hepatic iron overload. J Magn Reson Imaging 2011;33(2):348–55.

[40] Noetzli LJ, Mittelman SD, Watanabe RM, Coates TD, Wood JC. Pancreatic iron and glucose dysregulation in thalassemia major. Am J Hematol 2012;87(2):155–60.
[41] Hankins JS, McCarville MB, Loeffler RB, Smeltzer MP, Onciu M, Hoffer FA, et al. R2* magnetic resonance imaging of the liver in patients with iron overload. Blood 2009;113(20):4853–5.
[42] Wood JC, Zhang P, Rienhoff H, Abi-Saab W, Neufeld EJ. Liver MRI is more precise than liver biopsy for assessing total body iron balance: a comparison of MRI relaxometry with simulated liver biopsy results. Magn Reson Imaging 2015;33(6):761–7.